



**HAL**  
open science

## Middle Jurassic tracks of sauropod dinosaurs in a deep karst cave in France.

Jean-David Moreau, Vincent Trincal, Emmanuel Fara, Louis Baret, Alain Jacquet, Claude Barbini, Rémi Flament, Michel Wienin, Benjamin Bourel, Amandine Jean

### ► To cite this version:

Jean-David Moreau, Vincent Trincal, Emmanuel Fara, Louis Baret, Alain Jacquet, et al.. Middle Jurassic tracks of sauropod dinosaurs in a deep karst cave in France.. *Journal of Vertebrate Paleontology*, 2019, 39 (6), pp.e1728286. 10.1080/02724634.2019.1728286 . hal-02986785

**HAL Id: hal-02986785**

**<https://hal.science/hal-02986785v1>**

Submitted on 8 Mar 2024

**HAL** is a multi-disciplinary open access archive for the deposit and dissemination of scientific research documents, whether they are published or not. The documents may come from teaching and research institutions in France or abroad, or from public or private research centers.

L'archive ouverte pluridisciplinaire **HAL**, est destinée au dépôt et à la diffusion de documents scientifiques de niveau recherche, publiés ou non, émanant des établissements d'enseignement et de recherche français ou étrangers, des laboratoires publics ou privés.



Distributed under a Creative Commons Attribution - NonCommercial 4.0 International License

Middle Jurassic tracks of sauropod dinosaurs in a deep karst cave from France

JEAN-DAVID MOREAU,<sup>\*,1</sup> VINCENT TRINCAL,<sup>2,3</sup> EMMANUEL FARA,<sup>1</sup> LOUIS  
BARET,<sup>4</sup> ALAIN JACQUET,<sup>4</sup> CLAUDE BARBINI,<sup>4</sup> REMI FLAMENT,<sup>5</sup> MICHEL  
WIENIN,<sup>6</sup> BENJAMIN BOUREL,<sup>7</sup> and AMANDINE JEAN<sup>7</sup>

<sup>1</sup> CNRS UMR 6282 Biogéosciences, Université de Bourgogne Franche-Comté, 6 boulevard Gabriel,  
21000 Dijon, France, [jean.david.moreau@gmail.com](mailto:jean.david.moreau@gmail.com); [emmanuel.fara@u-bourgogne.fr](mailto:emmanuel.fara@u-bourgogne.fr);

<sup>2</sup> LMDC, Université de Toulouse, INSA/UPS, 135 avenue de Rangueil, 31077 Toulouse, France

<sup>3</sup> IMT Lille Douai, Université de Lille, Département GCE, Ecole des Mines, 764, boulevard Lahure,  
59508 Douai, France, [vincenttrincal@gmail.com](mailto:vincenttrincal@gmail.com);

<sup>4</sup> Association Paléontologique des Hauts Plateaux du Languedoc, 14 chemin des Ecureuils, 48000  
Mende, France, [louisbaret@netc.fr](mailto:louisbaret@netc.fr); [alainjacquet48@hotmail.com](mailto:alainjacquet48@hotmail.com); [barbini.claude@sfr.fr](mailto:barbini.claude@sfr.fr);

<sup>5</sup> SARL Jardin des Arts, 12 rue Pannessac, 43000 Le Puy-en Velay, France, [verticavite@gmail.com](mailto:verticavite@gmail.com);

<sup>6</sup> Parc National des Cévennes, Place du Palais, 48400 Florac, France, [michel@wienin.com](mailto:michel@wienin.com);

<sup>7</sup> Aix Marseille Univ, CNRS, IRD, INRA, Coll France, CEREGE, Aix-en-Provence, France,  
[bourel@cerege.fr](mailto:bourel@cerege.fr); [jean@cerege.fr](mailto:jean@cerege.fr)

\* Corresponding author.

RH: MOREAU ET AL.—SAUROPOD TRACKS IN A KARST FROM FRANCE

ABSTRACT—Although the deep galleries of natural underground cavities are difficult to access and are sometimes dangerous, they have the potential to preserve trace fossils. Here, we report on the first occurrence of sauropod dinosaur tracks inside a karstic cave. Three trackways are preserved on the roof of the Castelbouc cave 500 m under the surface of the Causse Méjean plateau (southern France). The tracks are Bathonian in age (about 168 to 166 million years), a crucial but still poorly-known time interval in sauropod evolution. The three trackways yield sauropod tracks that are up to 1.25 m long and are therefore amongst the largest known dinosaur footprints worldwide. The trackmakers are hypothesized to be titanosauriforms. Some of the tracks are extremely well preserved and show impressions of digits, digital pads and claws. We erect the new ichnogenus and ichnospecies *Occitanopodus gandi* igen. et isp. nov. In order to characterize depositional environments, sedimentological, petrographic and mineralogical analyses were conducted. The tracks from Castelbouc attest the presence of sauropods in proximal littoral environments during the Middle Jurassic. This discovery demonstrates the great potential of prospecting in deep karst caves that can occasionally offer larger and better-preserved surfaces than outdoor outcrops.

## INTRODUCTION

The Middle Jurassic was a crucial period in sauropod evolution as it corresponds to the interval just preceding to the Upper Jurassic large radiation of Neosauropoda (Upchurch and Martin, 2003; Mannion et al., 2019). However, bones of Middle Jurassic sauropods are extremely sparse throughout the world (Weishampel et al., 2004; Mannion et al., 2019). In this context, tracksites are precious evidence to reconstruct the evolution of this dinosaur group during this important time period.

Although sauropod tracks are relatively common in the Lower and Upper Jurassic of Europe, they remain extremely rare in Middle Jurassic deposits. Occurrences have been reported from Aalenian-Bathonian tracksites in Denmark (Milàn, 2011; Milàn and Bromley, 2005), Portugal (Santos et al., 1994, 2009), Scotland (Brusatte et al., 2015) and the United Kingdom (Romano et al. 1999; Day et al., 2002, 2004). In France, the putative Middle Jurassic sauropod tracks described by Sciau et al. (2006) have been reinterpreted as erosion structures and traces of trunks by Gand et al. (2007, 2018). Thus, definitive Middle Jurassic sauropod tracks have hitherto been unknown in France, whereas rare theropod trackways are reported from this geological interval (Sciau, 2006; Moreau et al., 2012; Moreau, 2017; Gand et al., 2018).

Here we report on Middle Jurassic sauropod trackways that were discovered during speleological prospecting in the Castelbouc karstic network (Causses Basin, southern France) (Figs. 1–2). Although dinosaur tracksites inside anthropic cavities (e.g., underground quarries or mines, railway tunnels) are well-known around the world (e.g., Peterson, 1924; Parker and Balsley, 1989; Ahlberg and Siverson, 1991; Lockley and Hunt, 1995; Belvedere et al., 2008; Cook et al., 2010), the discovery of dinosaur tracks inside a natural karstic cave is extremely rare (e.g., theropod tracks from the Hettangian deposits of the Bramabiau and Malaval Caves in southern France; Ellenberger, 1988; Moreau et al., 2018). The trackways from Castelbouc represent the first occurrence of sauropod tracks inside a natural karstic cave.

## HISTORICAL AND GEOLOGICAL CONTEXT OF THE CAVE

The Castelbouc karstic network is located in the northern part of the Causses Basin, 500 m under the surface of the Causse Méjean plateau (Lozère Department; Fig. 2A). Entrances to the network are located in the Gorges du Tarn, 30 km south of Mende (André,

1992). The Castelbouc caves have probably been known since pre-Medieval times (André, 1992). They are well-known locally for flooding after rainy events. They consist of two large caves (Castelbouc caves N°1 and N°4) and two karst springs (Castelbouc caves N°2 and N°3). The dinosaur tracks presented here are located in cave N°4. In 1952, the known part of the Castelbouc N°4 cavity was limited to a first gallery called the “Sous-Préfet” gallery (Fig. 2A). After many excavations since 1952, this cave is now 880 m long and exhibits 102 m of difference in elevation (André, 1992). The first dinosaur tracks were discovered by one of us (JDM) in 2015 during a speleological trip. Three scientific missions were organized in 2016, 2017 and 2018. Tracks are located on the roof of the Tunnel gallery (Fig. 2). This large gallery is 76 m long, up to 22 m wide and up to 11.5 m high. The access to the Tunnel gallery is only possible by crawling along very narrow labyrinthine conduits about 100 m long. Since some portions of these small conduits periodically flood, access to the far galleries requires caution and is limited to drought periods.

The Castelbouc N°4 Cave occurs in the “Calcaires à stipites” Formation, which is between 30 to 150 m thick in this area (Charcosset et al., 1996; Ciszak et al., 1999). It consists of grey limestone alternating with thin layers of lignitic marl, and white oolitic limestone. Regionally, in the southern part of the Causses Basin, lenticular lignitic beds of the “Calcaires à stipites” Formation were mined for coal (Rouire, 1946). Based on ammonites, brachiopods and foraminiferans, this formation is considered to be lower to upper Bathonian in age (Charcosset, 2000; Gand et al., 2018 and references therein).

## METHODS

In order to characterize depositional environments, sedimentological, petrographic, and mineralogical analyses were conducted along a 9-m-thick stratigraphic section accessible in the Tunnel gallery. Nine samples were prepared on standard polished thin sections for both optical microscopy (with a Zeiss Axiozoom macroscope) and mineralogical analyses.

### **XRD-Mineralogy**

Powders (thoroughly dried and micronized by grinding in an agate mortar and pestle) were analyzed using a Bruker D8 Advance diffractometer system using Co-K $\alpha$  radiation equipped with a fast LynxEye position sensitive detector (WL = 1.78897). The diffractometer was operated at 35 kV and 40 mA. Scans were run from 5° to 80°2 $\theta$ , with a step interval of 0.02°2 $\theta$  and a time acquisition of 96 s per step. The identification of minerals was performed using Bruker-AXS's DiffracPlus EVA software and the ICDD (the International Centre for Diffraction Data) Powder Diffraction File 2015 database.

Mineral quantification of the rock samples was made by Rietveld analysis (e.g., Bish and Post, 1993) with the DIFFRACplus TOPAS software, version 4.2 (Bruker-AXS). The Rietveld method consists of minimizing the difference between an experimental diffractogram and a diffractogram calculated for a given starting model. Crystal structure data were taken from the ICDD PDF and Bruker Structure Database. Rietveld refined parameters used in this study are the same as described in Trincal et al. (2014). Standard deviations of mineral contents were obtained by the multiplication of the standard deviation given by Topas software by the GOF (goodness of fit) in order to provide a more realistic approximation of error (Taylor and Hinczak, 2003; Trincal et al., 2014). However, it must be kept in mind that this method does not evaluate amorphous phases but only well-crystallised ones detected by XRD.

The percentage of amorphous vs. crystallised minerals was estimated by the simple qualitative method as advocated in the Bruker Eva software using the following formulas (1 and 2):

$$\%Amorphous = \frac{Global\ area - Reduced\ area}{Global\ area} * 100 \quad (1)$$

$$\%Crystallinity = 100 - \%Amorphous \quad (2)$$

where the global area includes all peaks and the ‘hump’ due to any X-ray amorphous material and the reduced area is the background subtracted scan, the subtraction including the amorphous ‘hump’.

### **Carbonate Quantification**

Thermogravimetry coupled with mass spectrometry analyses (TGA-MS) were conducted using a Netzsch STA449F3 Jupiter thermal analyser coupled with a Netzsch QMS403D Aëlos quadrupole mass spectrometer. Setup was configured for a temperature increase of 3°C/minute from 100 to 1000°C under an argon stream. This method, well adapted for sedimentary rocks (e.g., Moreau et al., 2018), measures quantitative mass loss and qualitative gas production generated by carbonate calcination. Since it includes amorphous phases, this method is complementary to the Rietveld quantifications.

### **XRF-Chemistry**

Bulk-rock chemical analyses were performed using a Bruker S4 Pioneer spectrometer, a 4 kW wavelength dispersive X-ray fluorescence spectrometer equipped with a rhodium

anode. Measurements were performed at 60 keV and 40 mA on powdered rock compressed tablets. The integrated standardless evaluation of the machine provides a fast and easy semi-quantitative determination of element concentrations down to the ppm-level without performing a calibration. Carbon was detected but not quantified with this method. XRF analyses were used for modal calculation following the method used in Trincal et al. (2014). This method consists in distributing all the chemical elements in the identified mineral phases and in quantifying them. As for ATG-MS, these estimates include the amorphous content of the rock (excluding organic matter), and could differ from results obtained by the Rietveld method. This method is used to qualitatively cross-validate previous results. Optical microscopy, X-ray fluorescence spectrometry (XRF), X-ray diffraction (XRD) and loss on ignition measures (on only one sample) were performed at the civil & environmental engineering department of Institut Mines Télécom Lille-Douai (Trincal et al., 2018).

### **Trace Fossil Analysis**

The descriptive terminology and biometric parameters used in this study follow Marty (2008). We used the following standard abbreviations (Fig. S1): PL, pedal track length; PW, pedal track width;  $\alpha$ , pedal track rotation; LPP, left pedal track pace length; RPP, right pedal track pace length; PS, pedal track stride length;  $\gamma$ , pedal track pace angulation; WAP, width of the pedal track angulation pattern or pes trackway width; pSW, pedal track side width; ML, manual track length; MW, manual track width;  $\beta$ , manual track rotation; LMP, left manual track pace length; RMP, right manual track pace length; MS, manual track stride length;  $\delta$ , manual track pace angulation; WAM, width of the manual track angulation pattern or manus trackway width; mSW, manual track side width; Dm-p, manual track-pedal track distance; iTW, inner trackway width; oTW, outer trackway width. The glenoacetabular distance (GA) that corresponds to the distance between the centre of the shoulder joint (glenoid cavity) and



the centre of the hip joint (acetabular cavity) was estimated by measuring the distance between the midpoint of a line connecting two consecutive pedal tracks (left and right or vice versa) and the midpoint of a line connecting the next two manual tracks (Fig. S1). Parameters were measured on the roof of the cave using a Leica DISTO X310 laser distance metre (precision of +/- 1 mm) combined with a Bosch Quigo Cross line laser. Measured values are listed in Table 2.

In addition to the parameters measured directly on tracks and trackways, several parameters were calculated. Following Thulborn (1990), index of pedal track size (IPS) was calculated using the formula  $(PL \times PW)^{0.5}$ , and index of manual track size (IMS) was calculated using the formula  $(ML \times MW)^{0.5}$ . Heteropody consists of the difference in area (total track area) between the pedal and manual tracks. The area of each track was calculated using the software ImageJ (version 1.43u; Schneider et al., 2012). According to Marty (2008), the trackway gauge was estimated using the pes trackway ratio PTR in equation 3:

$$PTR = \frac{\text{side width (SW)}}{\text{overall width (OW)}} * 100\% \quad (3)$$

with wide-gauge <40%< medium-gauge <50%< narrow-gauge, and the WAP/PL ratio with narrow-gauge <1.0< medium-gauge <1.2< wide-gauge.

Based on Alexander's (1976) formula (equation 4), the locomotion speed (v) was estimated using the calculated hip height (h) and the measured value of stride length (S) as follows:

$$v = 0.25g^{0.5} \times S^{1.67} \times h^{-1.17} \quad (4)$$

As explained by Salisbury et al. (2017), the glenoacetabular length typically exceeds osteological hip height in early sauropodomorphs, and although these two lengths converge in later sauropods (Paul, 2010), hip height rarely exceeds glenoacetabular distance. Following Salisbury et al. (2017), the hip height was estimated using the length of the glenoacetabular distance.

### **Photogrammetry**

In order to produce photogrammetric 3D reconstructions of the gallery and orthoimages of the track-bearing surface, the software Agisoft PhotoScan Professional 1.2.4 was used to align and combine multiple digital photographs taken by a Nikon D5200 camera coupled with an AF-S NIKKOR 18–105 mm f/3.5–5.6G ED camera lens. The same software was used to produce photogrammetric 3D textured meshes. Shadows were applied on 3D reconstructions using the MeshLab 1.3.2 software (Cignoni et al., 2008). The 3D meshes are available online on the open access database <https://figshare.com>.

## **RESULTS**

### **Stratigraphy and Petrography**

The stratigraphic column exposed in the Tunnel gallery displays limestone beds alternating with fossiliferous lenticular clayey layers (Fig. 3). Three lignitic lenses and three main erosive surfaces have been identified (S1-S3). We distinguish seven facies, F1 to F7 (see Table 1 and Figs. 3, 4). F1 consists of grey marl yielding fossil plants such as leafy axes of conifers. F2 is a grey to blue cryptalgal limestone showing abundant thin laminites with mud cracks and microbial mats (Fig. 4A). F3 consists of grey to blue limestone (a pelbiomicrite)

with marine bioclasts (Fig. 4B). F4 is a green, brown to black marly and coaly breccia. F4 corresponds to the facies overlying erosion surfaces S1-S3. F5 consists of lignitic and bioclastic marl yielding abundant marine remains. F6 is a grey/blue marly limestone (facies F6-Type A; Fig. 4C) locally bearing centimetric to decimetric black lignitic and oolitic, oncoidic to peloidic lenses yielding abundant intraclasts and bioclasts (bivalve shells, corals, foraminiferans and spines of sea-urchins) (facies F6-Type B) with short lateral extensions (Fig. 4D–E). F7 consists of grey oolitic limestone (oopelmicrite to peloomicrite) with abundant marine bioclasts as well as rare wood micro-remains (Fig. 4F).

## **Mineralogy**

Rietveld mineralogical quantifications indicate that the crystallized fraction is very homogenous, with more than 92 weight% of calcite, less than 5 wt% of illite/muscovite, less than 2 wt% of quartz and dolomite, and less than 1 wt% of rutile (Figs. S2–S4 and Tables S1–S3). The sample S3F6A (marly limestone) is distinguished by 82 wt% of calcite and 15 wt% of illite/muscovite, but this difference is not found laterally in S4F6B (lignitic marly limestone). Gypsum was identified only in sample S4F6B, with almost 1 wt%. The percentage of crystallinity ranges from 80 to 88 wt% in all samples. The remaining 12 to 20 wt% can be attributed to organic matter and/or to poorly crystallized minerals. Organic matter was detected by XRF in all samples and observed on thin section mainly in the sample S4F6B (Fig. 4). Its content was quantified at 2.25 wt% by loss on ignition in sample S4F6B. The ratio of crystallinity to illite/muscovite content suggests that the more phyllosilicates there are, the higher the “amorphous” content. Modal calculations performed with XRF data as well as calcite quantification by TGA-MS (Figs. S3–S4 and Tables S2–S4) suggest that calcite is slightly overvalued at the expense of other minerals, especially in clayed facies. All these

elements are consistent with the hypothesis that the amorphous fraction is enriched with small and poorly crystallized illite/muscovite at the expense of carbonates.

### **Tracks and their preservation**

The roof of the Tunnel gallery bears three trackways of sauropods (CAS-1, for trackway Castelbouc 1; CAS-2, for trackway Castelbouc 2; CAS-3, for trackway Castelbouc 3; Figs. 5–8). This surface is located at a height of 7.9 to 10.9 m above the floor of the cavern. We distinguish two trackway morphologies: quadrupedal, wide-gauge trackways (CAS-1 and CAS-2) and pedal track-only, narrow-gauge trackways (CAS-3). All of them can be classified as large sauropod trackways (pedal track length > 75 cm) according to the size classes proposed by Marty (2008).

The tracks occur at the interface of a marly limestone bed locally showing lignite lenses (facies F6; Fig. 3) and a pelomicrite bed containing abundant marine organisms (F7). Due to erosion of the marly limestones, concave epireliefs are not preserved. Only the infilled convex hyporeliefs are preserved on the roof of the cave (facies F7; Fig. 3).

The preservation of tracks is variable among the three trackways. Trackway CAS-1 shows well-preserved pedal and manual tracks. The outlines of the tracks composing CAS-2 are weakly marked and not complete. Several parameters cannot be definitively measured on this trackway (Table 2). The pedal track-only trackway CAS-3 shows exquisite details of claws and pads.

## SYSTEMATIC PALEOICHOLOGY

*OCCITANOPODUS GANDI*, igen. et isp. nov.

(Figs. 5–6; Fig. S5)

**Etymology**—The ichnogenus is derived from the « Occitanie » Region. The ichnospecies is dedicated to the French paleoichnologist Pr. Georges Gand.

**Holotype**—Manual track- pedal track set LM1-LP1 of the trackway CAS-1 preserved in situ on the roof of the Castelbouc N°4 Cave (Lozère, southern France).

**Locality, Horizon and Age**—The tracksite occurs in the Tunnel gallery of the Castelbouc N°4 Cave. Middle Jurassic, Bathonian, “Calcaires à Stipites” Formation.

**Diagnosis**— Ichnotaxon showing a combination of characters not observed amongst other wide-gauged sauropod tracks such as *Brontopodus*, *Polyonyx* and *Titanopodus* as well as medium- to wide-gauged sauropod tracks such as *Calorckosauripus* and *Oobardjidama*.

Trackway: wide-gauged sauropod trackway with pronounced heteropody (manual track area 4 to 6 times smaller than pedal track area). Pedal tracks and manual tracks aligned. Pedal tracks: form a small positive rotation angle relative to the trackway axis (0–27°). Large sized (about 1 m in length), pentadactyl, asymmetric, subcircular to oval pedal tracks. Pedal tracks mainly as long as wide or slightly wider than long. Maximum width of pedal tracks located in the middle, or slightly toward the anterior part of the track. Pedal tracks with short digit impressions that show strong outward rotation. Manual tracks: form a small positive rotation angle relative to the trackway axis (0–27°). Manual tracks symmetrical, D-shaped lacking any indication of digits or claws.

**Description**—The trackway CAS-1 is straight, about 18 m long, 2.6 m wide and includes twelve pedal tracks and ten manual tracks (at least five strides; Fig. 5). Since the WAP/PL ratio is between 1.2 and 2, and the PTR value is 39%, the trackway CAS-1 can be considered wide-gauged. The pedal tracks and the manual tracks are aligned on both sides of the midline trackway. Pedal track and manual track stride length are 3.2–3.5 m long and 3.1–

3.5 m long, respectively. Pedal track and manual track paces are very similar, being both 2.0–2.3 m long. Heteropody is pronounced though not constant along the trackway (1:4 to 1:6). Most of pedal tracks show a small positive rotation angle relative to the trackway axis ( $\alpha = 0\text{--}27^\circ$ ). The pedal tracks are asymmetric, subcircular to oval in shape and pentadactyl (Fig. 6). Pedal tracks are mainly as long as wide, with variable length and width within and between trackways. Pedal tracks are 56–94 cm long and 82–116 cm wide (IPS = 77–100). In most pedal tracks, the maximum width is located in the middle, or slightly toward the anterior part of the track. Traces of digits are very short and are strongly rotated outward. Most of manual prints show a small positive rotation angle with the trackway axis ( $\beta = 0\text{--}27^\circ$ ). Outlines of manual tracks are well-marked and do not seem to be deformed by the pedal tracks. The manual prints are symmetric, D-shaped and always convex forward. They are wider than long. They are 21–47 cm long and 40–76 cm wide (IMS = 33–53). Digit impressions are not marked.

**Remarks**—The PTR value suggests that CAS-1 is not so far from the medium-gauge category ( $40\% < \text{PTR} < 50\%$ ) defined in Marty (2008). As seen in some manual track-pedal track sets (e.g., LM1-LP1), the manual track is clearly distinct from the pedal track, showing that the high heteropody values cannot be explain by the overlap of manual imprints by pedal tracks. The glenoacetabular distance of the trackmaker is estimated to 2.3 to 2.7 m. We estimated the hip height of the trackmaker to 2.5 m.

## UNDETERMINED SAUROPOD TRACKS

### The Quadrupedal Wide-Gauge Trackway CAS-2

**Description**—CAS-2 trackway is about 15 m long, and includes at least seven pedal tracks (two complete and five partial) and three manual tracks (Fig. 5). The trackway is straight at its start and then is slightly curved to the right. Heteropody is pronounced (1:3 to

1:4). Pedal track stride and manual track stride lengths are 3.2–3.6 m long. The pedal tracks are asymmetric, mainly oval, wider than long. Pedal tracks are 65–98 cm long and 96–109 cm wide (IPS = 83–104). The manual prints are symmetric, crescent-shaped to D-shaped and always convex forward. They are wider than long. They are 23–31 cm long and 79–81 cm wide (IMS = 34–50). Neither the manual tracks nor the pedal tracks show impressions of digits.

**Remarks**—The trackway being poorly preserved, we refrain from assigning CAS-2 to an ichnotaxon. CAS-2 differs from *Occitanopodus gandi* igen. et isp. nov. in showing a smaller heteropody.

### **The Pes-Only Narrow Gauge Trackway CAS-3**

**Description**—CAS-3 trackway is 5.2 m long, 2.1 m wide and includes three large pedal tracks (Fig. 8; Fig. S6). Manual tracks are absent. Based on a WAP/PL ratio of 0.8, as well as a PTR value up to 51 %, the trackway can be considered as a narrow-gauged trackway. Pedal track stride length is 4.4 m long. Pedal track pace is 2.25–2.39 m long. Pedal tracks show a pronounced positive rotation angle with the trackway axis ( $\alpha = 26\text{--}40^\circ$ ). The pedal tracks are asymmetric, subtriangular in shape, longer than wide, pentadactyl, 119–125 cm long and 99–102 cm wide (IPS = 110–112). The maximum width of each pedal track is located toward the anterior part of the track. Pedal tracks exquisitely preserve impressions of digits and claws. Traces of digits are quite short, triangular in shape, longer than wide and strongly rotated outward. Digits I and II are better marked than digits III-IV. Distally, digit I shows an oval pad impression (Fig. 8C; Fig. S6).

**Remarks**—Although manual tracks are not observed in CAS-3, narrow-gauged trackways with pedal tracks intersecting the trackway midline are characteristic of two Middle to Upper Jurassic sauropod tracks: *Breviparopus* Dutuit and Ouazzou, 1980 and

*Parabrontopodus* Lockley et al., 1994. Although Wright (2005) suggested that *Parabrontopodus* may be a junior synonym of *Breviparopus*, Marty et al. (2010) considered both ichnotaxa valid. Although CAS-3 shares some similarities with *Breviparopus* (large pedal track length; large pedal track rotation up to 30°; pronounced heteropody; claw marks), it differs from this ichnogenus in showing a well-marked fifth digit. The manual tracks being missing, we refrain from assigning CAS-3 to an ichnotaxon.

## DISCUSSION

### **Preservation of the Tracks**

Similarly to trackway CAS-3, pedal track-only trackways are frequent in sauropod tracksites (e.g., Marty, 2008; Falkingham et al., 2011). It was sometimes explained by relatively small manual tracks being overprinted by subsequent, considerably larger pedal tracks (Marty, 2008). Alternatively, some sauropods may have been able to have an occasional bipedal stance over short distances (Wilson and Carrano, 1999). However, in most cases, the absence of manual tracks can be explained by preservational processes. When the foot does not penetrate the sediment but compresses it, it creates a stack of transmitted prints (stack of casts and moulds *sensu* Marty, 2008) called undertracks. They consist of more or less modified versions of the “true” tracks depending of the vertical distance from the tracking surface (Marty, 2008). The pressures exerted by the manus and pes being different (Falkingham et al., 2011), the deformation of the sediment is sometimes shallower below the tracked surface of the manus. It explains why some sauropod trackways only display pedal tracks. The tracks from Castelbouc not being visible in cross section, we cannot confidently determine if some of the tracks are actually undertracks.



The presence of a pedal track-only trackway as well as the various quality of preservation between CAS-1, CAS-2 and CAS-3 potentially suggest multiple track-bearing surfaces on and above the roof of the cave. If the walking surface of the pedal track-only CAS-3 is located above the roof of the cave, the exquisite details of claws and pads suggest that the “true” walking surface for this trackway was probably located very close to the roof. For trackway CAS-1 (*Occitanopodus gandi* igen. et isp. nov), the good preservation of pedal and manual tracks suggests that they are “true” tracks. Being located at the interface between the roof and the underlying bed (eroded in the Tunnel gallery), these tracks can be considered as natural moulds.

### **Comparison of *Occitanopodus* igen. nov. with Other Tracks**

Worldwide, Middle Jurassic sauropod trackways are ascribed to *Breviparopus* Dutuit and Ouazzou, 1980, *Brontopodus* Farlow et al., 1989, *Parabrontopodus* Lockley et al., 1994 and *Polyonyx* Santos et al., 1994. In Europe, although tracks remain unnamed in most Middle Jurassic tracksites, *Breviparopus*- and *Brontopodus*-like tracks were reported from the Aalenian of England (Yorkshire; Romano et al., 1999), and *Polyonyx gomesi* from the Bajocian-Bathonian of Portugal (Santos et al., 1994, 2009).

*Breviparopus* was erected based on Middle to Upper Jurassic trackways from Morocco (Dutuit and Ouazzou, 1980). This ichnogenus differs from *Occitanopodus* in showing narrow-gauge trackways with pedal tracks intersecting the trackway midline (like CAS-3), manual tracks are located further away from the midline than pedal tracks, and it has a lower heteropody (i.e. 1:3).

*Brontopodus* was described based on material from the Lower Cretaceous of the United States of America (*B. birdi*; Farlow et al., 1989). *B. birdi* and *O. gandi* igen. et isp.

nov. share some similarities like wide-gauge trackway, large size of pedal tracks (i.e. up to 100 cm), and clawless manual track. However, they are distinguished for the following reasons. *B. birdi* differs in having pedal marks clearly longer than wide, as long as wide U-shape manual prints that show rounded marks on digits I and V, and a lower heteropody (i.e. 1:3 among *B. birdi*; Lockley et al., 1994). *Brontopodus pentadactylus* from the Lower Cretaceous of Korea clearly differs from *Occitanopodus* in having outwardly rotated manual prints and a lower heteropody (i.e. 1:2; Kim and Lockley, 2012). *Brontopodus plagnensis* from the lower Tithonian of eastern France differs in showing a long, sharp antero-lateral claw mark pointing postero-laterally on the impression of pedal digit V (Mazin et al., 2017).

*Parabrontopodus* was erected based on material from the Upper Jurassic of the United States of America (Lockley et al., 1994). In France, this ichnogenus was reported from the lower Kimmeridgian and the Tithonian from the Jura Department (Le Loeuff et al., 2006; Mazin et al., 2016). Although *Parabrontopodus* show medium to large sized tracks (i.e. 50–90 cm), strong heteropody (i.e. 1:4 or 1:5 in *P. mcintoshi*; Lockley et al., 1994), and manual track wider than long, this ichnogenus differs from *Occitanopodus* in showing narrow-gauge trackway characterized by the absence of space between the trackway midline and the inside margin of the pedal tracks. In addition, pedal tracks are longer than wide, with the long axis rotated outward.

Although *Polyonyx gomesi* consists of wide-gauge trackway with large pedal tracks (i.e. PL = 90–95, PW = 60–70), this ichnotaxon differs from *Occitanopodus* by low heteropody (1:2); asymmetric manual track with a large claw mark on the impression of digit I that is posteriorly oriented (Santos et al., 1994).

Excluding several ichnotaxa currently regarded as *nomina dubia* (Lockley et al., 1994; Wright, 2005), another ichnotaxon showing wide-gauge trackways was reported from the

Upper Cretaceous of Argentina, *Titanopodus mendozensis* González Riga and Calvo, 2009. *T. mendozensis* differs from *Occitanopodus* by the outer limits of the trackway that are defined in some cases by manual prints, smaller tracks, lower heteropody (i.e. 1:3) and manual prints strongly rotated outward (i.e. 25–48°; González Riga and Calvo, 2009). The medium- to wide-gauge trackway *Oobardjidama foulkesi* was described from the Cretaceous deposits of Australia (Salisbury et al., 2017). *O. foulkesi* mainly differs from *Occitanopodus* by a lower heteropody (30–45%), a smaller manual angulation (69–74°), and pedal tracks with a lobed medial margin. Recently, Meyer et al. (2018) described *Calorckosauripus lazari* from the Late Cretaceous deposits of Bolivia. This wide/intermediate-gauge trackway with strong heteropody (1:1.85) differs from *Occitanopodus* by small size of the tracks (PL = 49 cm and PW = 42 cm), lower value of PTR (22-34%), pedal tracks always longer than wide and absence of digit impressions on pedal tracks.

*Occitanopodus gandi* igen. et isp. nov. (trackway CAS-1) shows a combination of characters not observed amongst other Jurassic and Cretaceous sauropod tracks (wide-gauge trackway with pronounced heteropody up to 1:6 ; large sized, as long as wide, pentadactyl, asymmetric, subcircular to oval pedal tracks with short digit impressions that show strong outward rotation; symmetrical, D-shaped manual tracks lacking any indication of digits or claws; pedal tracks and manual tracks forming a small positive rotation angle relative to the trackway axis).

### **Possible Trackmakers**

The record of Middle Jurassic sauropod body fossils is very sparse worldwide (Weishampel et al., 2004; Mannion et al., 2017). In Europe, sauropod skeletal remains from this epoch were mainly reported from the Aalenian-Callovian of England (e.g., Manning et al., 2015) and the Bathonian of Scotland (e.g., Clark et al., 1995; Barrett, 2006; Clark and

Gavin, 2016). Bathonian-Callovian sediments from France only yield rare sauropod remains (Sauvage, 1900; Buffetaut, 1995; Buffetaut et al., 2011). Although the “Calcaires à stipites” Formation yielded some dinosaur teeth ascribed to ornithopods and theropods (Kriwet et al., 1997), sauropod body fossils are unknown in the Bathonian, as well as in any other Jurassic deposits from the Causses Basin. Some isolated bones and teeth ascribed to undetermined sauropods were reported from the Bathonian of the Indre Department and from the lower Callovian of Calvados, in northwestern France (Buffetaut, 1995). Only a lower Bathonian chevron bone from Les Ardennes Department was attributed to the eusauropod *Cetiosaurus* (Buffetaut et al., 2011). *Cetiosaurus* was reported from several Middle and Upper Jurassic localities in England (e.g., Owen, 1841; Benton and Spencer, 1995; Upchurch and Martin, 2003). According to Upchurch and Martin (2003:208), *Cetiosaurus* lies outside of, but is closely related to, the clade Neosauropoda.

The identity of the trackmakers of wide-gauge trackways has been debated for some time and is still problematic (Farlow, 1992; Wilson and Carrano, 1999). Many authors attributed wide-gauge trackways to brachiosaurids or titanosaurids (e.g., Wilson and Carrano, 1999; Day et al., 2002, 2004; Wilson, 2005), both included in the clade Titanosauriformes (Wilson and Sereno, 1998; Wilson and Carrano, 1999). For example, according to Wilson (Wilson, 2005:408), the most common ichnotaxon showing wide-gauge trackways, *Brontopodus*, was likely made by a titanosauriform or possibly by saltosaurids, two clades originating in the Middle Jurassic and in the Early Cretaceous, respectively (Wilson, 2005). In contrast, Santos et al. (2009) proposed that wide-gauge trackways are not exclusive to Titanosauriformes and that *Polyonyx* was made by non-neosauropod eusauropods. Overall, it seems that the trackway gauge is not a reliable indicator of the trackmakers. Indeed, there are instances in which a single trackway changes from wide to narrow gauge (Leonardi and Avanzini, 1994; Wilson, 2005). Moreover, Lockley et al. (2002:395) suggested that

titanosaurids may have changed from narrow gauge to wide gauge during growth. According to some authors (e.g. Marty et al., 2010; Meyer et al., 2018), gauge was probably influenced by behavior (different degrees of lateral bending, speed) or sexual dimorphism.

Manual tracks of *Occitanopodus* do not show any evidence of a large claw print on digit I (like tracks assigned to *Polyonyx*). It is not consistent with the predicted manual track morphology for diplodocoids and basal macronarians (Day et al., 2002; Wright, 2005). In contrast, titanosauriforms have reduced ungual phalanges on the manus (Day et al., 2004). The claw of digit I is reduced among brachiosaurs (i.e. *Brachiosaurus*), whereas it is missing among titanosaurids (Upchurch, 1994). Thus, despite an uncertainty, the best candidate for the trackmakers of *Occitanopodus* is a titanosauriform. They are known from the Middle Jurassic to the Upper Cretaceous and measured more than 30 m long and weighed more than 50 tons for the largest (Paul, 2010). In the absence of skeletal remains for this period in France, the tracks from Castelbouc may represent the first evidence of titanosauriforms in this area during the Middle Jurassic. This report complements the few other Middle Jurassic European tracksites yielding titanosauriform tracks (e.g. Day et al., 2002, 2004; Santos et al., 2009) and suggests that although the main radiation of the clade occurred during the Late Jurassic (Mannion et al., 2019), Titanosauriformes were probably present as early as the Middle Jurassic.

### **Palaeoenvironmental Reconstruction**

The presence of brachiopods, benthic foraminiferans, corals and echinoids in the Castelbouc stratigraphic section attests that the depositional environments were in part marine. However, lignite beds yielding cuticles of conifers, woods and terrigenous minerals (phyllosilicates, quartz and rutile) indicate terrestrial inputs. In the context of the second main low sea-level of the Tethys during the Jurassic filling of the Causses Basin, the co-occurrence

of marine and terrestrial organisms suggests that the Castelbouc stratigraphic series was deposited in a panel of marginal-littoral palaeoenvironments with possible brackish to euhaline conditions (Table 1). The surfaces bearing mud cracks and dinosaur trackways, as well as the main erosive surfaces indicate that sediments were deposited in very proximal environments with a thin layer of water and which were occasionally emerged.

Based on field observations associated with microfacies and mineralogical analyses, we identified various depositional environments (Table 1). They include (from the most proximal to the most distal): protected backshore areas not open to the sea (Facies F1), intertidal to supratidal zones periodically emerged (Facies F2); borders of bay or lagoon showing co-occurrence of strong marine and terrestrial inputs (possible brackish conditions) (Facies F5-F6); and foreshore (beach) to shoreface domains (Facies F3-F4 and F7). Preservation of tracks suggests that the “true” walking surfaces are located in F6 and F7. Whereas F7 clearly exhibits strong marine influence, the lignitic marly limestone of F6 suggests a shallow paralic environment commonly restricted but occasionally open to the sea. The depositional environment of F6 was periodically emerged and recorded occasional hydrodynamic events such as storms reworking material from the sea and transporting it into the paralic depositional environment. The sauropods from Castelbouc walked along beaches open to the sea and bays or a lagoons sometimes affected by storms and floods that concentrated large amounts of plant remains locally. The occurrence of gypsum in Facies F6B suggests evaporitic conditions but we cannot exclude that it is a newly formed karstic mineral.

Plant cuticles collected in the Tunnel gallery suggest the presence of a conifer-dominated forest along the coastline trampled by sauropods. All palaeobotanical studies of the “Calcaires à Stipites” Formation revealed plant macro-remains, pollen, spores, and woods that attest diversified and abundant floras in freshwater to brackish littoral environments of the Causses Basin (Doubinger, 1961; Alabouvette et al., 1988; Philippe et al., 1998). Such a

vegetation was probably an attractive and important source of food for megaherbivorous dinosaurs. During the early to middle Bathonian, the regional climate was semi-arid, changing to arid later in the Bathonian (Philippe et al., 1998).

Over the last decades, bone micro-remains (Kriwet et al., 1997), as well as ichnological record (Sciau et al., 2006; Moreau et al., 2012; Moreau, 2017; Gand et al. 2018) suggested that Middle Jurassic environments from the Causses Basin were inhabited by dinosaur communities composed of ornithischians and theropods. The new tracks from Castelbouc attest the presence of giant sauropods in proximal littoral ecosystems, similarly to what is observed in other Middle Jurassic tracksites (e.g. Castanera et al., 2014; Brusatte et al., 2015; dePolo et al., 2018). This discovery demonstrates the high potential for palaeoichnological prospecting in deep karst caves that can sometimes offer larger and better preserved rocky surfaces than outdoor outcrops.

## CONCLUSION

The Bathonian sauropod tracks from the Castelbouc cave consist of three trackways including two quadrupedal, wide-gauge trackways and one pedal track-only, narrow-gauge, trackway. The new ichnotaxon *Occitanopodus gandi* igen. et isp. nov. (trackway CAS-1) shows a combination of characters not observed amongst other Jurassic and Cretaceous sauropod tracks. Stratigraphy, petrology and mineralogy show that the sediments exposed in the Tunnel gallery were deposited in very proximal environments with a thin layer of water and that were occasionally emerged. The tracksite from Castelbouc attests the presence of large sauropods such as Titanosauriformes in littoral environments during the Middle Jurassic. This report suggests that, although the main radiation of the clade occurred during

the Late Jurassic, the Titanosauriformes were probably already present in Middle Jurassic ecosystems.

#### ACKNOWLEDGEMENTS

We thank Michael D’Emic, S. Salisbury, P. dePolo and an anonymous reviewer for their constructive and thoughtful reviews on the manuscript. We thank G. Dumont and J. Dupont for technical assistance during photographic sessions. We express our gratitude to the Bouty family, owner of the entrance of the cave, who authorized the access to the cavity. We thank D. André, D. Bosc as well as J.-C. Dufour for discussions and information about the cavity. We also thank J. Caboche and D. Betrancourt, from the IMT Lille-Douai, for their contribution to mineralogical analyses. We express our gratitude to G. Gand who provided constructive comments on the manuscript. This publication is a contribution to the project “Empreintes de dinosaures de la Grotte Castelbouc N°4” led by the A.P.H.P.L. (Mende, Lozère).

#### LITERATURE CITED

Ahlberg, A., and M. Siverson. 1991. Lower Jurassic dinosaur footprints in Helsingborg, southern Sweden. *Geologiska Föreningens i Stockholm Förhandlingar* 113:339–340.



- Alabouvette, B., J. P. Arrondeau, M. Aubague, Y. Bodeur, P. Dubois, J. Mattei, H. Paloc, and J. P. Rançon. 1988. Notice explicative de la feuille Le Caylar à 1/50 000. BRGM, Orléans.
- Alexander, R., McN. 1976. Estimates of speeds of dinosaurs. *Nature* 261:129–130.
- André, D. 1992. Lozère des ténèbres. Spéléo Club de la Lozère, Saint-Georges-de-Luzençon, 257 pp.
- Barrett, P. M. 2006. A sauropod dinosaur tooth from the Middle Jurassic of Skye, Scotland. *Earth and Environmental Science Transactions of the Royal Society of Edinburgh* 97:25–29.
- Belvedere, M., P. Mietto, M. Avanzini, and M. Rigo. 2008. Norian dinosaur footprints from the “Strada delle Gallerie”(Monte Pasubio, NE Italy). *Studi Tridentini Scienze Naturali, Acta Geologica* 83:267–275.
- Benton, M. B., and P. S. Spencer. 1995. Fossil reptiles of Great Britain. Chapman & Hall, London, 386 pp.
- Bish, D. L., and J. E. Post. 1993. Quantitative mineralogical analysis using the Rietveld full-pattern fitting method. *The American Mineralogist* 78:932–940.
- Brusatte, S. L., T. J. Challands, D. A. Ross, and M. Wilkinson. 2015. Sauropod dinosaur trackways in a Middle Jurassic lagoon on the Isle of Skye. *Scottish Journal of Geology* 52:1–9.
- Buffetaut, E. 1995. Un dinosaure sauropode dans le Callovien du Calvados (Normandie, France). *Bulletin trimestriel de la Société géologique de Normandie et des amis du Muséum du Havre* 82:5–11.
- Buffetaut, E., B. Gibout, I. Launois, and C. Delacroix. 2011. The sauropod dinosaur *Cetiosaurus* OWEN in the Bathonian (Middle Jurassic) of the Ardennes (NE France): insular, but not dwarf. *Carnets de Géologie* CG2011\_L06:149–161.

- Castanera, D., Vila, B., Razzolini, N. L., Santos, V. F., Pascual, C., and Canudo, J. I., 2014, Sauropod trackways of the Iberian Peninsula: Palaeoetological and palaeoenvironmental implications: *Journal of Iberian Geology* 40:49–59.
- Charcosset, P. 2000. Synthèse paléogéographique et dynamique du bassin caussenard (Sud de la France) au cours du Bathonien (Jurassique moyen). *Eclogae Geologicae Helvetiae* 93:53–64.
- Charcosset, P., R. Ciszak, B. Peybernès, and J. -P. Garcia. 1996. Modalités séquentielles de la transgression bathonienne sur le "Seuil cévenol" (Grands Causses). *Comptes Rendus Académie des Sciences de Paris* 323:419–426.
- Ciszak, R., B. Peybernès, J. Thierry, and P. Faure. 1999. Synthèse en termes de stratigraphie séquentielle du Dogger et de la base du Malm dans les Grands Causses. *Géologie de la France* 4:45–58.
- Clark, N. D., and P. Gavin. 2016. New Bathonian (Middle Jurassic) sauropod remains from the Valtos Formation, Isle of Skye, Scotland. *Scottish Journal of Geology* 52:71–75.
- Clark, N. D. L., J. D. Boyd, R. J. Dixon, and D. A. Ross. 1995. The first Middle Jurassic dinosaur from Scotland: a cetiosaurid?(Sauropoda) from the Bathonian of the Isle of Skye. *Scottish Journal of Geology* 31:171–176.
- Cignoni, P., M. Callieri, M. Corsini, M. Dellepiane, F. Ganovelli, and G. Ranzuglia. 2008. Meshlab: an open-source mesh processing tool; pp. 129–136 in V. Scarano, R. De Chiara, and U. Erra (eds.), *Eurographics Italian chapter conference*. Eurographics Asso., Geneve.
- Cook, A.G., N. Saini, and S. A. Hocknull. 2010. Dinosaur footprints from the Lower Jurassic of Mount Morgan, Queensland. *Memoirs of the Queensland Museum* 55:135–146.

- Day, J. J., P. Upchurch, D. B. Norman, A. S. Gale, and H. P. Powell. 2002. Sauropod trackways, evolution, and behavior. *Science* 296:1659–1659.
- Day, J. J., D. B. Norman, A. S. Gale, P. Upchurch, and H. P. Powell. 2004. A Middle Jurassic dinosaur trackway site from Oxfordshire, UK. *Palaeontology* 47:319–348.
- dePolo, P. E., S. L. Brusatte, T. J. Challands, D. Foffa, D. A. Ross, M. Wilkinson, and H.-Y. Yi. 2018. A sauropod dominated tracksite from Rubha nam Brathairean (Brothers' Point), Isle of Skye, Scotland: *Scottish Journal of Geology* 54:1–12.
- Doubinger, J. 1961. Spores et pollens des 'stipites' du Larzac (Bathonien). *Compte Rendu Sommaire des Séances de la Société Géologique de France*:162–163.
- Dutuit, J. -M., and A. Ouazzou. 1980. Découverte d'une piste de dinosaure sauropode sur le site d'empreintes de Demnat (Haut Atlas marocain). *Mémoires de la Société géologique de France* 139:95–102.
- Ellenberger, P. 1988. La découverte des pistes de dinosauriens de Camprieu. *Causses et Cévennes* 7:139–140.
- Falkingham, P. L., K. T. Bates, L. Margetts, and P. L. Manning. 2011. Simulating sauropod manus-only trackway formation using finite-element analysis. *Biology Letters* 7:142–145.
- Farlow, J. O. 1992. Sauropod tracks and trackmakers: integrating the ichnological and skeletal records. *Zubía*, 10:89–138.
- Farlow, J. O., J. G. Pittman, and J. M. Hawthorne. 1989. *Brontopodus birdi*, Lower Cretaceous sauropod footprints from the U. S. Gulf coastal plain; pp. 371–394 in D.D. Gillette, and M.G. Lockley (eds.), *Dinosaur Tracks and Traces*. Cambridge University Press, Cambridge.

- Gand, G., G. Demathieu, and C. Montenat. 2007. Les traces de pas d'amphibiens, de Dinosaures et autres Reptiles du Mésozoïque français: inventaire et interprétations. *Palaeovertebrata* 35:1–149.
- Gand, G., E. Fara, C. Durllet, G. Caravaca, J. -D. Moreau, L. Baret, D. André, R. Lefillatre, A. Passet, M. Wiénin, J. -P. Gély. 2018. Les pistes d'archosauriens : *Kayentapus ubacensis* nov. isp. (théropodes) et crocodylomorphes du Bathonien des Grands-Causse (France). Conséquences paléo-biologiques, environnementales et géographiques. *Annales de Paléontologie* 104:183–216.
- González Riga, B. J., J. O. Calvo. 2009. A new wide-gauge sauropod track site from the late Cretaceous of Mendoza, Neuquén Basin, Argentina. *Palaeontology* 52:631–640.
- Kim, J. Y., and M. G. Lockley. 2012. New sauropod tracks (*Brontopodus pentadactylus* ichnosp. nov.) from the Early Cretaceous Haman Formation of Jinju Area, Korea: implications for sauropods manus morphology. *Ichnos* 19:84–92.
- Kriwet, J., O. W. M. Rauhut, and U. Gloy. 1997. Microvertebrate remains (Pisces, Archosauria) from the Middle Jurassic (Bathonian) of southern of France. *Neues Jahrbuch für Geologie und Paläontologie* 206:1–28.
- Le Lœuff, J., C. Gourrat., P. Landry, L. Hautier, R. Liard, C. Souillat, E. Buffetaut, R. Enay. 2006. A Late Jurassic sauropod tracksite from southern Jura (France). *Comptes Rendus Palevol* 5:705–709.
- Leonardi, G., and M. Avanzini. 1994. Dinosauri in Italia. *Le Scienze, Quaderni* 76:69–81.
- Lockley, M. G., and Hunt, A. P. 1995. Ceratopsid tracks and associated ichnofauna from the Laramie Formation (Upper Cretaceous: Maastrichtian) of Colorado. *Journal of Vertebrate Paleontology* 15:592–614.

- Lockley, M. G., J. O. Farlow, and C. A. Meyer. 1994. *Brontopodus* and *Parabrontopodus* ichnogen. nov. and the significance of wide- and narrow-gauge sauropod trackways. *Gaia* 10:135–146.
- Lockley, M. G., A. S. Schulp, C. A. Meyer, G. Leonardi, and D. K. Mamani. 2002. Titanosaurid trackways from the Upper Cretaceous of Bolivia: evidence for large manus, wide-gauge locomotion and gregarious behaviour. *Cretaceous Research* 23:383–400.
- Manning, P. L., V. M. Egerton, and M. Romano. 2015. A new sauropod dinosaur from the Middle Jurassic of the United Kingdom. *PloS one* 10(6), e0128107.
- Mannion, P. D., Upchurch, P., Schwarz, D., and O. Wings. 2019. Taxonomic affinities of the putative titanosaurs from the Late Jurassic Tendaguru Formation of Tanzania: phylogenetic and biogeographic implications for eusauropod dinosaur evolution. *Zoological Journal of the Linnean Society* 185:784–909.
- Marty, D. 2008. Sedimentology, taphonomy, and ichnology of Late Jurassic dinosaur tracks from the Jura carbonate platform (Chevenez-Combe Ronde tracksite, NW Switzerland): insights into the tidal-flat palaeoenvironment and dinosaur diversity, locomotion, and palaeoecology. *Geofocus* 21:1–278.
- Marty, D., M. Belvedere, C. A. Meyer, P. Mietto, G. Paratte, C. Lovis, and B. Thüring. 2010. Comparative analysis of Late Jurassic sauropod trackways from the Jura Mountains (NW Switzerland) and the central High Atlas Mountains (Morocco): implications for sauropod ichnotaxonomy. *Historical Biology* 22:109–133.
- Mazin, J. -M., P. Hantzpergue, and J. Pouech. 2016. The dinosaur tracksite of Loulle (early Kimmeridgian; Jura, France). *Geobios* 49:211–228.

- Mazin, J. -M., P. Hantzpergue, and N. Olivier. 2017. The dinosaur tracksite of Plagne (early Tithonian, Late Jurassic; Jura Mountains, France): The longest known sauropod trackway. *Geobios* 50:279–301.
- Meyer, C.A., D. Marty, and M. Belvedere. 2018. Titanosaur trackways from the Late Cretaceous El Molino Formation of Bolivia (Cal Orck'o, Sucre). *Annales Societatis Geologorum Poloniae* 88:223–241.
- Milà, J. 2011. New theropod, thyreophoran, and small sauropod tracks from the Middle Jurassic Bagå Formation, Bornholm, Denmark. *Bulletin of the Geological Society of Denmark* 59:51–59.
- Milà, J., and R. G. Bromley. 2005. Dinosaur footprints from the Middle Jurassic Bagå Formation, Bornholm, Denmark. *Bulletin of the Geological Society of Denmark* 52:7–15.
- Moreau, J. -D. 2017. Des empreintes de dinosaures dans le Bathonien du Causse de Sauveterre. *Bulletin de la Société des Lettres, Sciences, et Arts de la Lozère* 44:75–81.
- Moreau, J.-D., L. Baret, G. Gand, E. Fara, C. Durllet, and G. Caravaca. 2012. Découverte d'un nouveau site à traces de pas de Dinosaures dans le Bathonien des Causses (Le Gayrand, Gorges de la Jonte, Lozère, France); pp. 13–19 in *Ichnologie dinosaurienne du Jurassique de Meyrueis*. Association Paléontologique des Hauts Plateaux du Languedoc, Mende.
- Moreau, J. D., V. Trincal, D. André, L. Baret, A. Jacquet, M. Wienin. 2018. Underground dinosaur tracksite inside a karst of southern France: Early Jurassic tridactyl traces from the Dolomitic Formation of the Malaval Cave (Lozère). *International Journal of Speleology* 47:29–42.

- Owen, R. 1841. A description of a portion of the skeleton of *Cetiosaurus*, a gigantic extinct saurian occurring in the Oolitic Formation of different parts of England. *Proceedings of the Geological Society of London* 3:457–62.
- Parker, L. R., and J. K. Balsley. 1989. Coal mines as localities for studying dinosaur trace fossils; pp. 353–359 in D.D. Gillette, and M.G. Lockley (eds.), *Dinosaur tracks and traces*. Cambridge University Press, Cambridge.
- Paul, G. S., 2010. *The Princeton Field Guide to Dinosaurs*. Princeton University Press, Princeton, 177 pp.
- Peterson, W. 1924. Dinosaur tracks in the roofs of coal mines. *Natural History* 24:388–397.
- Philippe, M., F. Thévenard, G. Barale, G. Guignard, and S. Ferry. 1998. Middle Bathonian floras and phytocoenoses of France. *Palaeogeography, Palaeoclimatology, Palaeoecology* 143:135–158.
- Romano, M., M. A. Whyte, and P. L. Manning. 1999. New sauropod dinosaur prints from the Saltwick Formation (Middle Jurassic) of the Cleveland Basin, Yorkshire. *Proceedings of the Yorkshire Geological and Polytechnic Society* 52:361–369.
- Rouire, L. 1946. Lignites du Larzac. Deuxième partie. *Mines et Concessions* 26:317–367.
- Salisbury, S. W., Romilio, A., Herne, M. C., Tucker, R. T., and J. P. Nair. 2017. The dinosaurian ichnofauna of the Lower Cretaceous (Valanginian-Barremian) Broome Sandstone of the Walmadany Area (James Price Point), Dampier Peninsula, Western Australia. *Journal of Vertebrate Paleontology* 36:1–152.
- Santos, V. F., J. J. Moratalla, and R. Royo-Torres. 2009. New sauropod trackways from the Middle Jurassic of Portugal. *Acta Palaeontologica Polonica* 54:409–422.

- Santos, V. F., M. G. Lockley, C. A. Meyer, J. Carvalho, A. M. Galopim de Carvalho, and J. J. Moratalla. 1994. A new sauropod tracksite from the Middle Jurassic of Portugal. *Gaia* 10:5–13.
- Sauvage, H. -E. 1900. Note sur les poissons et les reptiles du Jurassique inférieur du département de l'Indre. *Bulletin de la Société Géologique de France* 28:500–504.
- Schneider, C. A., W. S. Rasband, and K. W. Eliceiri. 2012. NIH Image to ImageJ: 25 years of image analysis. *Nature Methods* 9:671–675.
- Sciau, J., M. Bécaud, and G. Gand. 2006. Présence de Dinosaures Théropodes et probablement d'Ornithopodes et de Sauropodes dans le marais maritime Bajocien-Bathonien des Causses. Association des Amis du Musée de Millau, Millau, 32 pp.
- Taylor, J. C., and I. Hinczak. 2003. Rietveld made easy: a practical guide to the understanding of the method and successful phase quantifications. Sietronics Pty Ltd, Canberra.
- Thulborn, T. 1990. *Dinosaur tracks*. Chapman & Hall, London, 410 pp.
- Trincal, V., D. Charpentier D, M. D. Buatier, B. Grobety, B. Lacroix, B. P. Labaume, and J.-P. Sizun. 2014. Quantification of mass transfers and mineralogical transformations in a thrust fault (Monte Perdido thrust unit, southern Pyrenees, Spain). *Marine and Petroleum Geology* 55:160–175.
- Trincal, V., Thiéry, V., Mamindy-Pajany, Y., and Hillier, S. 2018. Use of hydraulic binders for reducing sulphate leaching: application to gypsiferous soil sampled in Ile-de-France region (France). *Environmental Science and Pollution Research International*, 25:22977–22997.
- Upchurch, P. 1994. Manus claw function in sauropod dinosaurs. *Gaia* 10:161–171.
- Upchurch, P., and J. Martin. 2003. The anatomy and taxonomy of *Cetiosaurus* (Saurischia, Sauropoda) from the Middle Jurassic of England. *Journal of Vertebrate Paleontology* 23:208–231.



- Weishampel, D. B., P. Dodson, and H. Osmólska. 2004. *The Dinosauria*. University of California Press, Berkeley.
- Wilson, J. A. 2005. Integrating ichnofossil and body fossil records to estimate locomotor posture and spatiotemporal distribution of early sauropod dinosaurs: a stratocladistic approach. *Paleobiology* 31:400–423.
- Wilson, J. A., and P. Sereno. 1998. Early evolution and higher level phylogeny of sauropod dinosaurs. *Journal of Vertebrate Paleontology* 18:1–68.
- Wilson, J. A., and M. T. Carrano. 1999. Titanosaurs and the origin of “wide-gauge” trackways: a biomechanical and systematic perspective on sauropod locomotion. *Paleobiology* 25:252–267.
- Wright, J. L. 2005. Steps in understanding sauropod biology – The importance of sauropod tracks; pp. 252–280 in K. A. Curry Rogers, and J. A. Wilson, (eds), *The sauropods: evolution and paleobiology*. University of California Press, Berkeley and Los Angeles.

Submitted October 12, 2018; accepted Month DD, YYYY.

TABLE 1. Microfacies.

No.	Facies	Textures	Description	Depositional environments
F1	Gray marl	M	Gray marl. Some leafy axes of conifers (compressions with cuticle) ascribed to <i>Brachyphyllum</i> sp. and <i>Pagiophyllum</i> sp.	Shallow environment not open to the sea (backshore?).
F2	Cryptalgal laminites	M (P)	Gray/blue limestone with abundant thin laminites. No bioclasts. Mud cracks. Microbial mats. Microbial laminae parallel to the bedding planes and wavy to planar. Nonporous fabric.	Intertidal to supratidal zone. Tidal flat. Periodic emersions.
F3	Bioclastic limestone	M-W(P)	Gray/blue bioclastic limestone (pelbiomicrite). Abundant peloids, some ooids. Bioclasts including bivalves, brachiopods, corals, foraminiferans, and gastropods. Burrows.	Shallow environment not far from the shore.
F4	Lignitic breccia	P	Coaly breccia with angular/subangular limestone blocs in green/brown/black clayey matrix.	Foreshore/beach. High hydrodynamism.
F5	Bioclastic marl	W(P)	Gray marl with thin layer of lignite yielding micro- and macroremains of wood. Bivalves, brachiopods. Rares <i>Lepidotes</i> scales.	Low-energy coastal environment, such as lagoon or enclosed bay.
F6	Lignitic oncoidic to peloidic marly limestone	M-W-P	Gray/blue or black marly limestone locally bearing centimetric to decimetric lignitic oncoidic to peloidic lenses with short lateral extensions. Abundant compressed woods, as well as fragments of bivalve shells, corals, foraminiferans, and spines of urchins. Intraclasts of oomicrite limestone.	Border of a shallow, restricted environment (bay or lagoon), periodically emerged or open to the sea. Brackish?
F7	Oolitic limestone	P(W)	Gray oolitic limestone and peloomicrite locally with abundant fragments of bivalves, brachiopods, corals, benthic foraminiferans (miliolids), and echinoids. Some microremains of wood.	Shoreface to foreshore. High energy shoals.

Abbreviations: M, mudstone; P, packstone; W, wackestone.

TABLE 2. Biometric data of sauropod trackways from Castelbouc.

Dimension	CAS-1		CAS-2		CAS-3	
	Average	Min-Max	Average	Min-Max	Average	Min-Max
Pedal track length (PL)	85	56–94	77	64–98	122	119–125
Pedal track width (PW)	102	82–116	103	96–109	100	99–102
Index of pedal track size (IPS)	92	77–100	89	83–104	111	110–112
Pedal track rotation ( $\alpha$ )	14°	0–27°	—	—	38°	26–40°
Manual track length (ML)	34	21–47	27	23–31	—	—
Manual track width (MW)	62	40–76	65	49–81	—	—
Index of manual track size (IMS)	45	33–53	41	34–50	—	—
Manual track rotation ( $\beta$ )	14°	0–27°	—	—	—	—
Trackway orientation	N290°	—	N130°	—	N125°	—
Pedal track stride length (PS)	334	320–346	341	325–357	440	—
Width of the pedal track angulation pattern (WAP)	128	116–141	—	—	100	—
Right pedal track pace length (RPP)	206	197–222	—	—	239	—
Left pedal track length (LPP)	225	216–230	—	—	225	—
Pedal track pace angulation ( $\gamma$ )	104°	—	—	—	128°	—
Pedal track side width (pSW)	102	82–116	103	96–109	102	98–108
Manual track stride length (MS)	323	310–348	341	341	—	—
Width of the manual track angulation pattern (WAM)	134	112–160	—	—	—	—
Right manual track pace length (RMP)	218	203–232	—	—	—	—
Left manual track pace length (LMP)	216	206–221	—	—	—	—
Manual track pace angulation ( $\delta$ )	100°	—	—	—	—	—
Manual track side width (mSW)	62	40–76	—	—	—	—
Outer trackway width (oTW)	—	260–270	—	—	210	—
Inner trackway width (itw)	—	30–40	—	—	—	—
Dm-p (manual track–pedal track distance)	77	55–105	60	52–68	—	—
WAP/PL	1.5	—	—	—	0.8	—
WAP/IPS	1.4	—	—	—	1.1	—
WAM/ML	3.9	—	—	—	—	—
WAP/IMS	2.8	—	—	—	—	—
Pedal trackway ratio (PTR)	39%	31–44%	—	—	49%	45–51%
Manual trackway ratio (MTR)	26%	22–30%	—	—	—	—
Glenoacetabular distance (GA)	249	230–270	—	—	—	—
Locomotion speed ( $v$ ; km/h)	7.2	—	—	—	—	—

Linear measurements in cm.

## FIGURE CAPTIONS

FIGURE 1. Photograph of the Tunnel gallery in the Castelbouc N°4 Cave (view from the East). By Rémi Flament. [planned for page width]

FIGURE 2. Castelbouc N°4 Cave and details of the gallery yielding dinosaur tracks. **A**, Location of the Causses Basin in France and topography of the cave showing the location of the Tunnel gallery. **B–C**, Photogrammetric 3D textured meshes of the part of the gallery yielding ichnofossils, in longitudinal E-W, section (**B**) and transversal N-S sections (**C**); red arrows indicate the surface bearing traces. **D–G**, Photogrammetric 3D meshes of the roof of the gallery yielding tracks in two different views, with (**E**, **G**) and without (**D**, **F**) texture. [planned for page width]

FIGURE 3. Stratigraphic section of the Tunnel gallery showing location of dinosaur tracks. **Abbreviations: Fac.**, facies; **Lith.**; lithology; **Sa.**, location of samplings; **Thi.**, thickness (m). [planned for page width]

FIGURE 4. Microfacies F2-F6. **A**, Cryptalgal laminites with micrite and sparite layers (F2). **B**, Pelbiomicrite showing stylolites (F3). **C**, Marly limestone (F6A). **D–E**, Lignitic marly limestone showing ooliths, oncoids, and peloids (F6B). **F**, Oopelmicrite (F7). [planned for page width]

FIGURE 5. Surface of the roof of the Tunnel gallery bearing sauropod trackways. **A–C**, Photogrammetric 3D textured mesh (**A**), photogrammetric 3D mesh using the “dimple” filter of the MeshLab software (**B**), and interpretative sketch (**C**). **D–E**, Detail of CAS-1 and CAS-2, showing a photogrammetric 3D mesh without texture (**D**) and interpretative sketch (**E**).  
[planned for page width]

FIGURE 6. *Occitanopodus gandi* igen. et isp. nov. **A–B**, Photograph of trackway CAS-1 (**A**) and interpretative sketch (**B**). **C–L**, Some pedal track-manual track sets of trackway CAS-1.  
[planned for page width]

FIGURE 7. Trackway CAS-2. **A**, Photogrammetric 3D textured mesh with texture. **B**, Interpretative sketch. [planned for page width]

FIGURE 8. Trackway CAS-3. **A**, Photogrammetric 3D textured mesh with texture. **B**, Interpretative sketch. **C**, Right feet of trackway CAS-3 (RP2'') showing traces of digits I-V.  
[planned for page width]

Figure 1



Figure 2

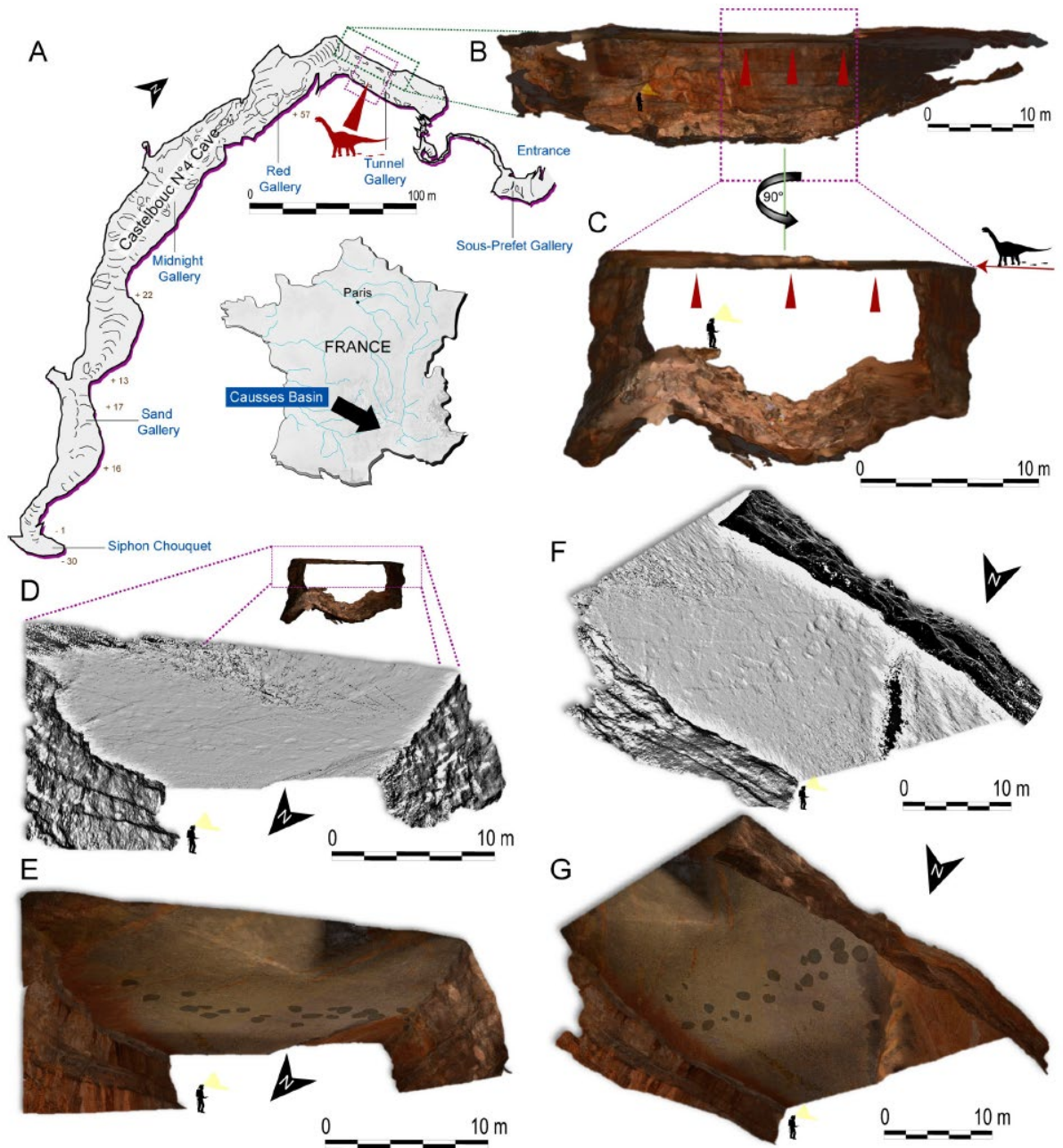


Figure 3

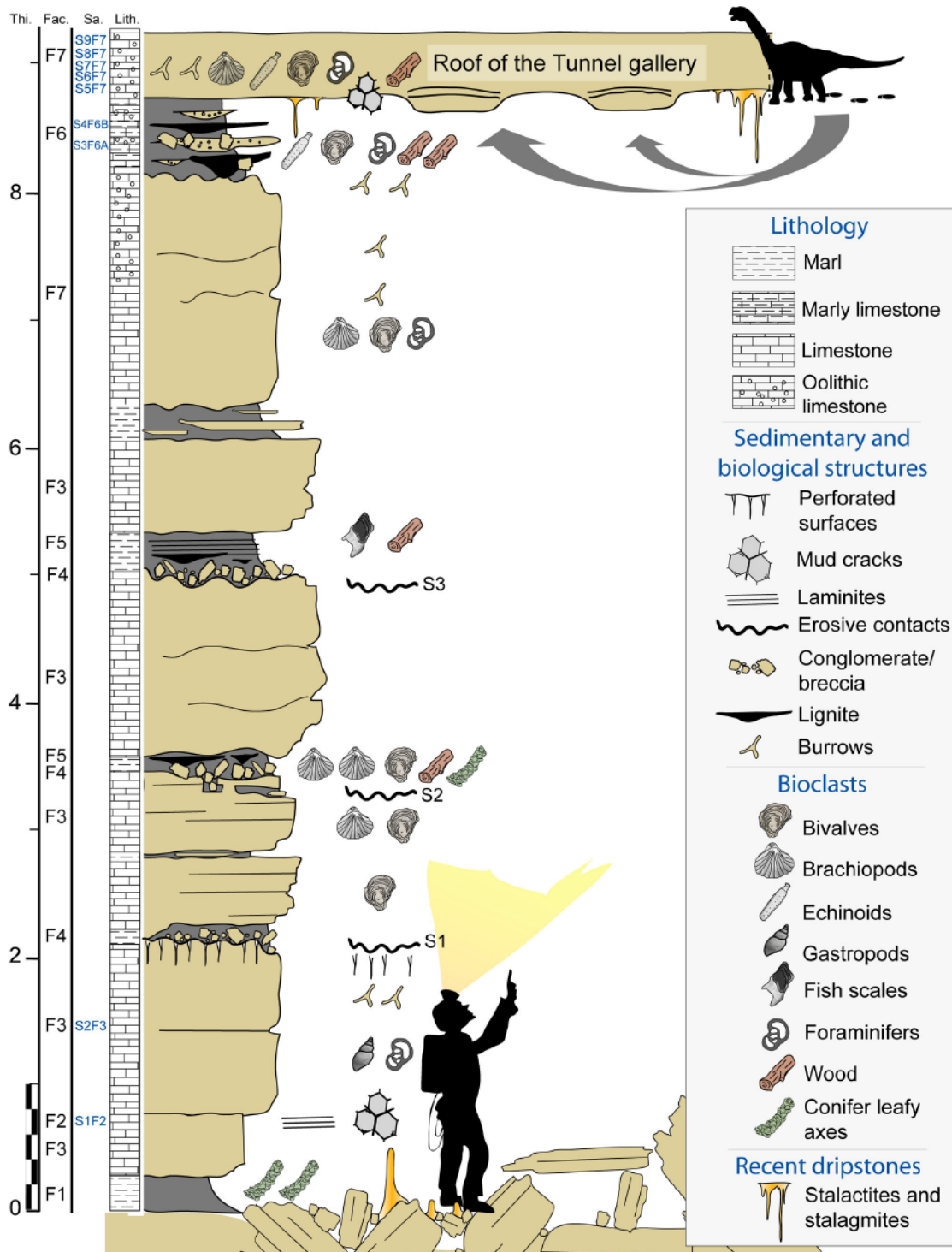


Figure 4

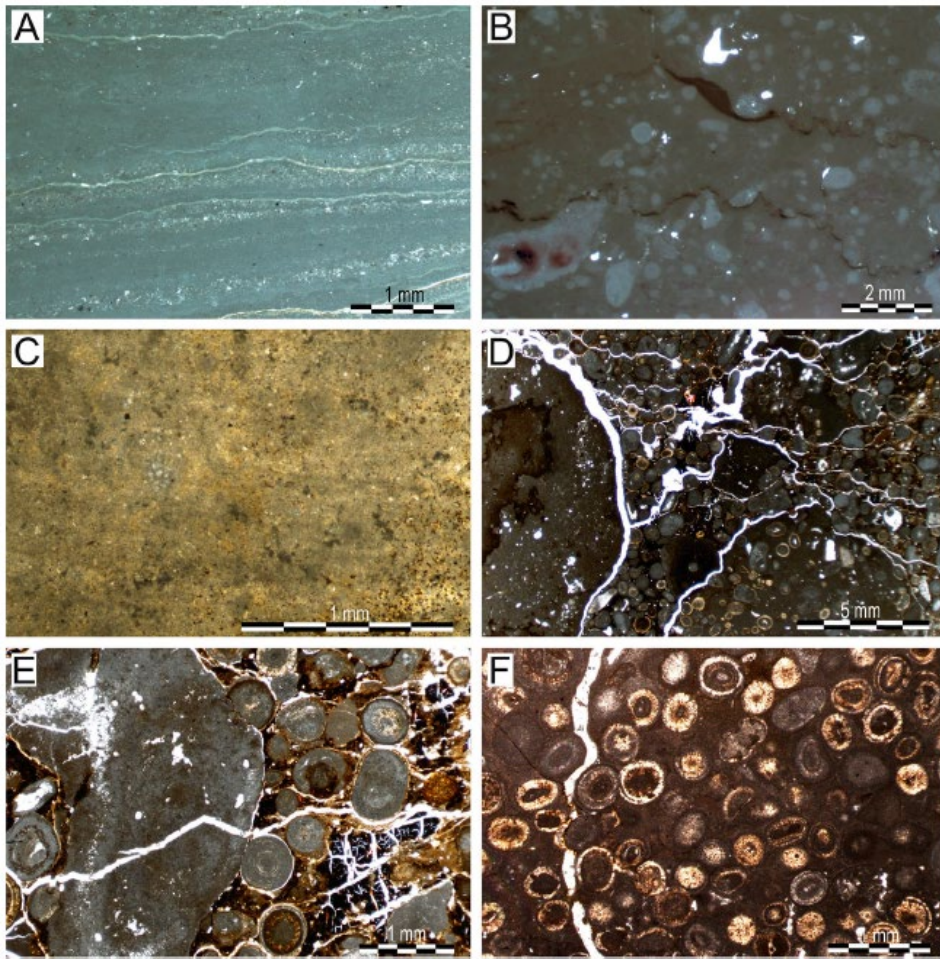


Figure 5

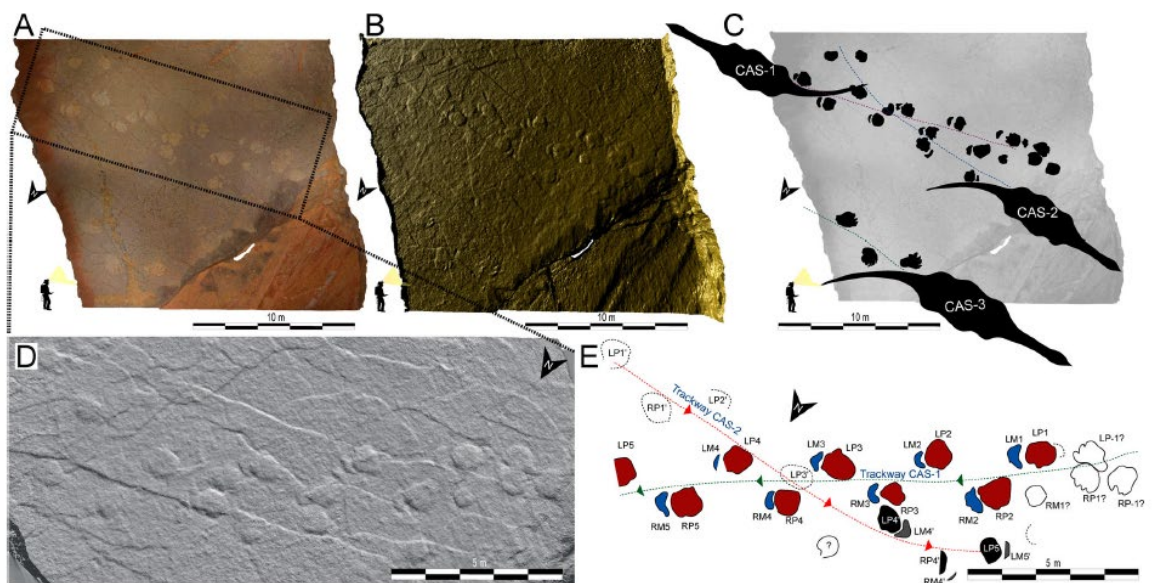




Figure 6

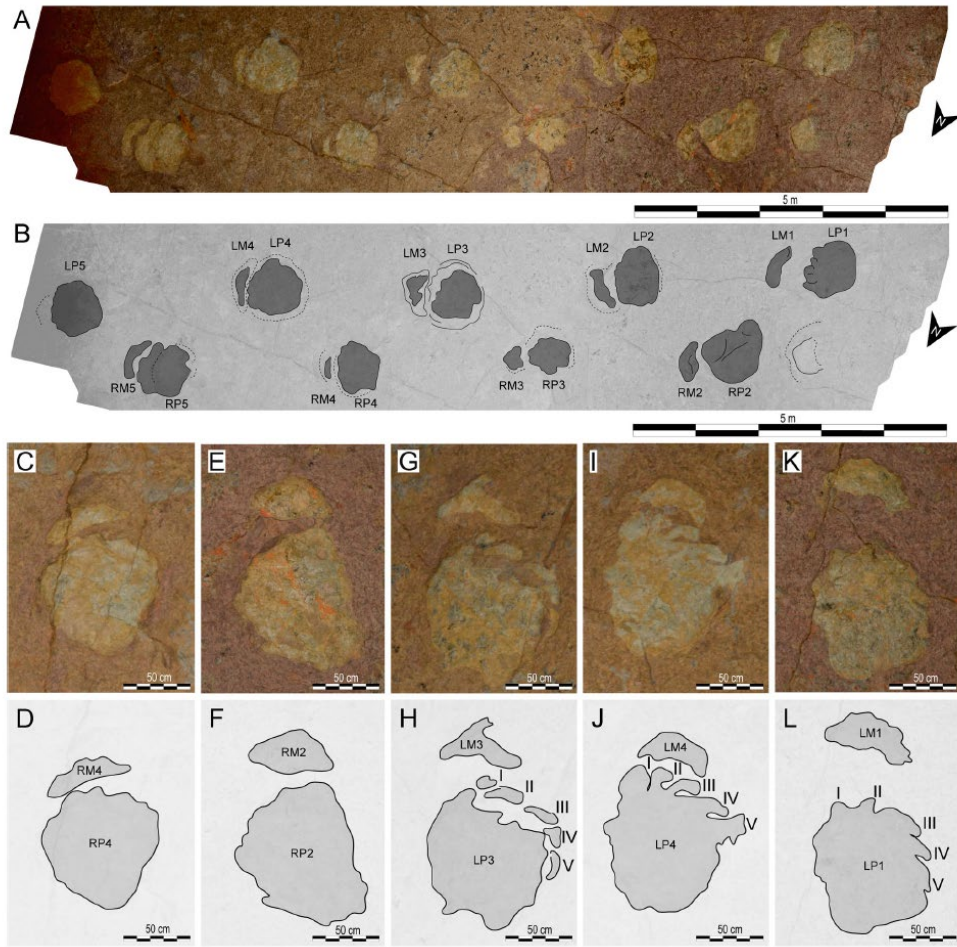


Figure 7

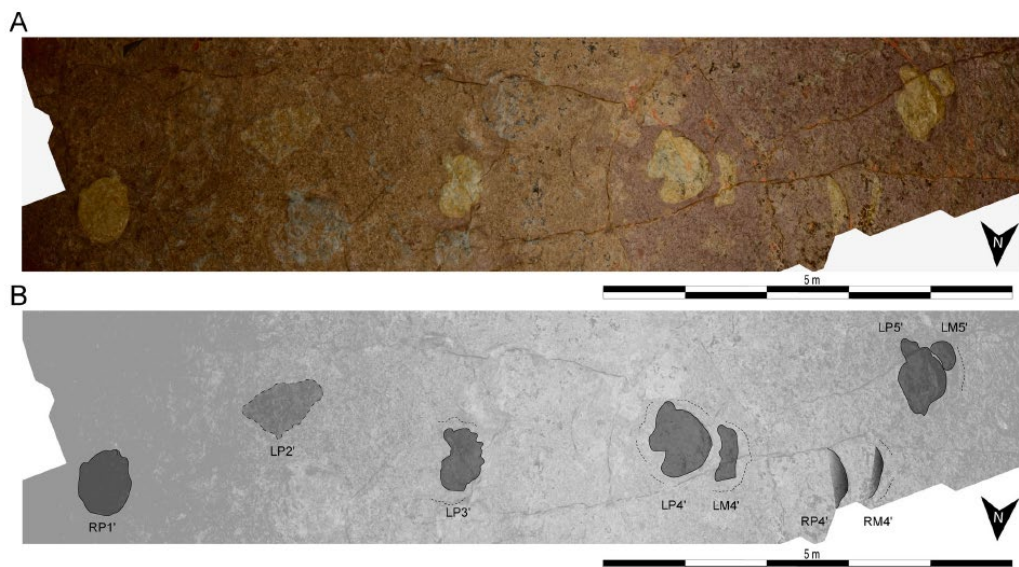


Figure 8

